

UDC 53.087- 577.391

## SYNTHESIS AND STRUCTURE OF YAG PHOSPHORS IN THE RADIATION FIELD

**A.B. Kukenova, G.K. Alpysova**

[aizat.kukenova@gmail.com](mailto:aizat.kukenova@gmail.com)

Postgraduate for special «Nanomaterials and nanotechnology» L.N.Gumilyev Eurasian National University, Nur-Sultan, Kazakhstan  
Supervisor – Usseinov A.B.

White light-emitting diodes (LEDs) are considered a good lighting devices due to their unsurpassed qualities, such as energy saving and long service life [1, 2]. In the most common LEDs, the blue radiation of the chip is converted into yellow by the phosphor. The combination of blue chip radiation and yellow phosphor gives white light. As phosphors, microcrystalline powders of yttrium-aluminum garnet (YAG:Ce), activated with cerium, are most often used [2–4].

YAG:Ce<sup>3+</sup> phosphor emits in the range of 500–700 nm, the luminescence maximum is 550 nm [5]. The quantum efficiency of YAG:Ce<sup>3+</sup> phosphor radiation can reach 85 % [6].

In recent years, radiation methods for modifying, synthesizing films and even ceramics have been developed [10, 11]. In this paper, it was attempted phosphor synthesis using powerful hard radiation fluxes. The surface, elemental composition, structure and luminescent characteristics of obtained YAG:Ce ceramics were studied.

### *1 Objects and research methods*

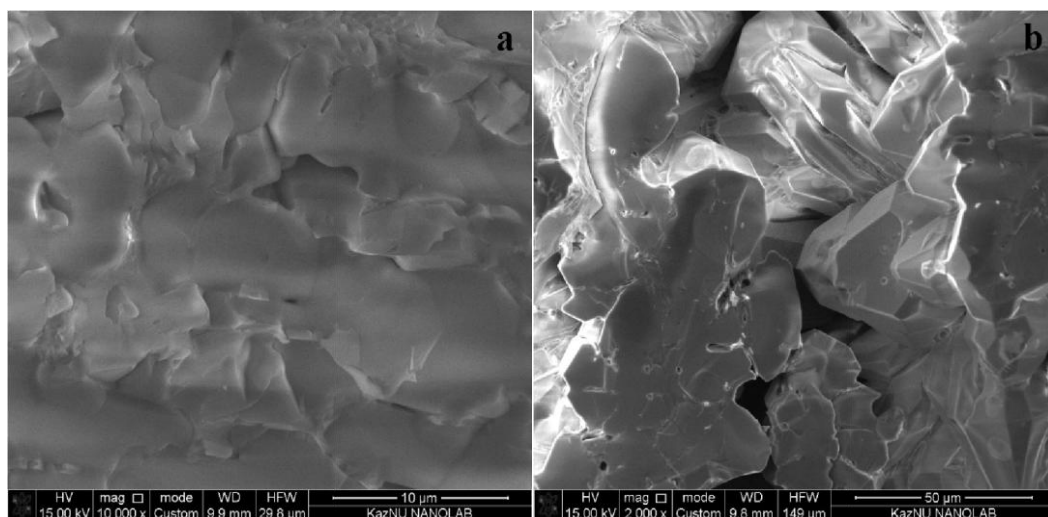
YAG:Ce and YAGG:Ce ceramics samples were synthesized in the radiation field. For the synthesis, a mixture from a powders mixture of Al<sub>2</sub>O<sub>3</sub>, Y<sub>2</sub>O<sub>3</sub>, Gd<sub>2</sub>O<sub>3</sub>, and Ce<sub>2</sub>O<sub>3</sub> oxides brands ch.c was prepared. The ratio of oxides in the charge was equal to stoichiometric. With cerium doping for activation and gadolinium for modification, the ratio of the initial compositions was adjusted. It was supposed that the activator and modifier ions enter the lattice by replacing yttrium ions. A flux of electrons with an energy of 1.4 MeV from the ELV-6 accelerator with an average power of 23 kW/cm<sup>2</sup> was directed to the melting pot with the charge. The beam section of a Gaussian shape at half-height was 0.7 cm<sup>2</sup>.

The state of the surface and the elemental composition of synthesized ceramics samples surface were studied using Hitachi TM-scanning electron microscope (SEM) 3030 with the Bruker X Flash MIN SVE energy dispersive analysis system at an accelerating voltage of 15 kV. X-ray diffraction analysis of synthesized ceramic samples was performed on a D8 ADVANCE ECO diffractometer with an X-ray tube with a copper anode and a graphite monochromator. Diffraction patterns were recorded in the range of angles (20–110°) 2θ with a step of 0.02 2θ. Quantitative phase dependence was determined in the TOPAS-4.2 program. The half-width of the measured reflections was used to determine the sizes of crystallites and microstresses in the sample. The ratio of the integral intensity of reflections to the total intensity of x-rays was used to evaluate the degree of crystallinity of the sample.

### *2 SEM images and elemental analysis of phosphors*

The morphology, elemental composition, structure obtained samples were investigated. In the chips SEM images it can be seen that the ceramic samples are soldered to each other particles with sizes of ~ 5...50 microns (Fig. 1). Most particles have a melt appearance. There are particles with a well-defined cut, which indicates about microcrystals formation.

The elemental composition of obtained YAG:Ce, YAGG: Ce samples differ from initial composition in charge. The proportion of aluminum ions exceeded the charge during the charge formation relative to Y, Ce, Gd. Therefore, the resulting ceramics has a non-stoichiometric composition (Tables 1, 2).



*a* — YAG:Ce; *b* — YAGG:Ce

Figure 1. The morphology of synthesized ceramics in a radiation field

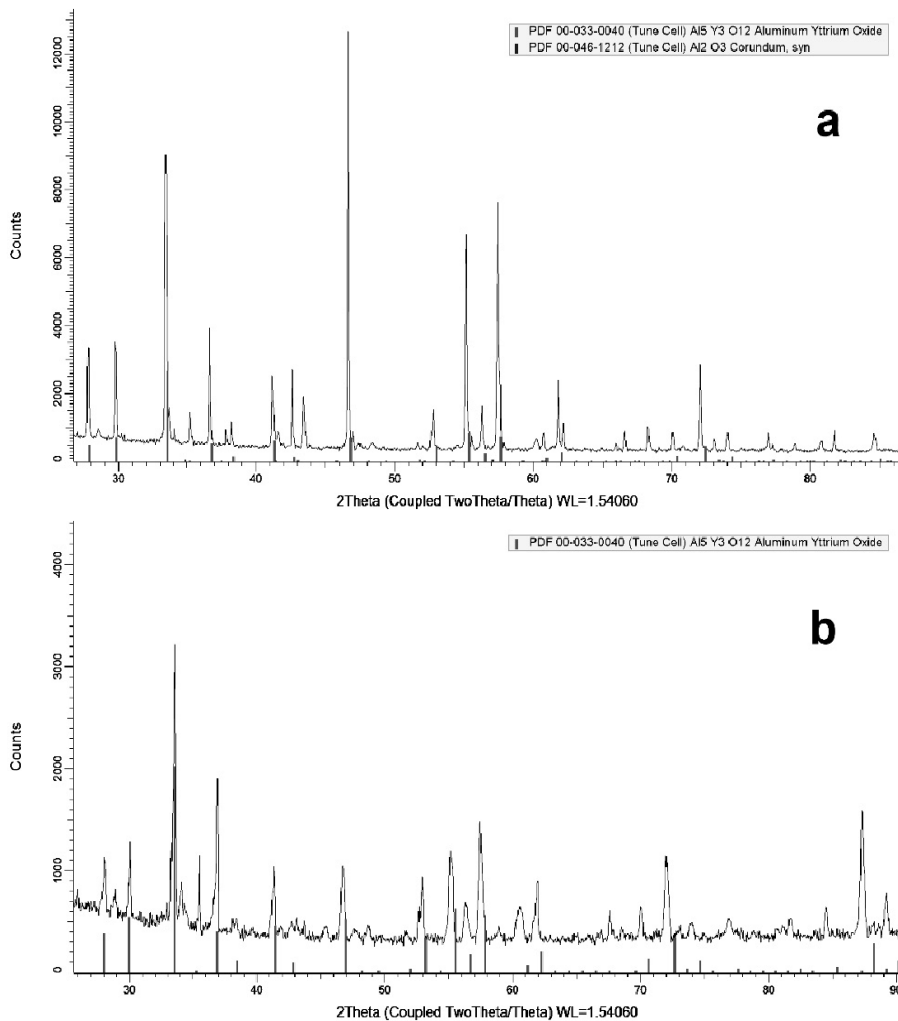
Table 1. The elemental composition of the surface of obtained samples of ceramics

Atom (at.%)	Al <sub>2</sub> O <sub>3</sub> (56,8 %) + Y <sub>2</sub> O <sub>3</sub> (34,1 %) + Ce <sub>2</sub> O <sub>3</sub> (9,1 %) (22 KBТ)	Al <sub>2</sub> O <sub>3</sub> (59,5 %) + Y <sub>2</sub> O <sub>3</sub> (35,7 %) + Ce <sub>2</sub> O <sub>3</sub> (4,8 %) (22 KBТ)	Al <sub>2</sub> O <sub>3</sub> (56,8 %) + Y <sub>2</sub> O <sub>3</sub> (22,7 %) + Gd <sub>2</sub> O <sub>3</sub> (11,4 %) + Ce <sub>2</sub> O <sub>3</sub> (9,1 %) (22 KBТ)	Al <sub>2</sub> O <sub>3</sub> (59,5 %) + Y <sub>2</sub> O <sub>3</sub> (23,8 %) + Gd <sub>2</sub> O <sub>3</sub> (11,9 %) + Ce <sub>2</sub> O <sub>3</sub> (4,8 %) (25 KBТ)
O	65.84	62.74	69.58	57.51
Al	26.16	33.02	28.72	36.36
Y	7.23	3.66	0.93	4.15
Ce	0.77	0.53	0.63	0.71
Gd	–	0.06	0.15	1.26

Table 2. The elemental composition of the crushed phosphor

Atom (at.%)	Al <sub>2</sub> O <sub>3</sub> (56,8 %) + Y <sub>2</sub> O <sub>3</sub> (34,1 %) + Ce <sub>2</sub> O <sub>3</sub> (9,1 %) (22 KBТ)	Al <sub>2</sub> O <sub>3</sub> (56,8 %) + Y <sub>2</sub> O <sub>3</sub> (22,7 %) + Gd <sub>2</sub> O <sub>3</sub> (11,4 %) + Ce <sub>2</sub> O <sub>3</sub> (9,1 %) (22 KBТ)	Al <sub>2</sub> O <sub>3</sub> (56,8 %) + Y <sub>2</sub> O <sub>3</sub> (34,1 %) + Ce <sub>2</sub> O <sub>3</sub> (9,1 %) (25 KBТ)
O	57.39	52.81	66.32
Al	33.26	37.76	25.65
Y	7.55	7.29	7.49
Ce	1.8	1.35	0.54
Gd	–	0.8	–

X-ray structural analysis showed that the resulting ceramics has a high degree of crystallinity, about 80 % (Fig. 2). The basis of YAG ceramics is made up of crystals with a size of 47 nm, YAGG — 81 nm. The existence of a separate phase of corundum was found in ceramics. The lattice parameters of YAG, YAGG, and Al<sub>2</sub>O<sub>3</sub> are close to those known for crystals: *a*, *b*, ≈12.023 in YAG, 12.055 in YAGG, 4.75 in Al<sub>2</sub>O<sub>3</sub> (Table 3).



*a* —  $\text{Al}_2\text{O}_3$  (59,5 %) +  $\text{Y}_2\text{O}_3$ (35,7 %) +  $\text{Ce}_2\text{O}_3$  (4,8 %); *b* —  $\text{Al}_2\text{O}_3$  (56,8 %) +  $\text{Y}_2\text{O}_3$  (22,7 %) +  $\text{Gd}_2\text{O}_3$  (11,4 %) +  $\text{Ce}_2\text{O}_3$  (9,1 %)

Figure 2. Diffractograms of the investigated samples

Thus, obtained ceramics is a system of small crystallites, which can be combined into microcrystals up to 50  $\mu\text{m}$ , has a dominant YAG (or YAGG) phase, the composition is close to the corresponding this phase, but non-stoichiometric.

#### 4 Conclusion

YAG:Ce ceramics first synthesized in the field of powerful flux of radiation. Ceramics has a heterogeneous structure. The main phase of obtained ceramics is YAG, which makes up from 72 to 91 % of the total volume of the samples. The remaining volume of samples consists of phases  $\text{Al}_2\text{O}_3$  and  $\text{CeO}_2$ . Synthesized ceramics has characteristics like a YAG:Ce, YAGG:Ce phosphors.

Thus, the synthesis of luminescent YAG:Ce, YAGG:Ce ceramics in a radiation field is possible. The advantages of this method are obvious. The synthesis time is 1 second. The efficiency of synthesis compared to the commonly used thermal is determined by ionization processes, but not by thermal ones. With used irradiation modes, during the exposure to the radiation flux, the charge absorbs  $6 \cdot 10^{23}$  eV/cm<sup>3</sup> in the charge,  $\sim 6 \dots 10^{22}$  cm<sup>-3</sup> electronic excitations (ions, excitons, electron-hole pairs) are creating. Consequently, the formation of structural phases occurs from a set of charge elements with a high degree of ionization, that is, from a state close to the plasma state. This provides good mixing of the elements of the composition, can be obtained ceramics with a composition close to stoichiometric. The radiation field, the distribution of the absorbed energy in the charge can be well controlled. Consequently, synthesis in the radiation field can provide high reproducibility of obtained materials.

## Literature

1. Kong, D.S., Kim, M.J., Song, H.J., Cho, I.S., Jeong, S., & Shin, et al. Fine tuning of emission property of white lightemitting diodes by quantum-dot-coating on YAG:Ce nanophosphors. *Appl. Surf. Sci.*- 379.- 2016.- 467–473.
2. Nakamura, S., Mukai, T., & Senoh, M. Candela-class high-brightness InGaN/AlGaN double-heterostructure blue-light-emitting diodes. *J. Appl. Phys.*- 1994.-Vol.76.-P. 1687–1689.
3. Xia, Z., & Meijerink, A. Ce<sup>3+</sup>-Doped garnet phosphors: composition modification, luminescence properties and applications. *Chem. Soc. Rev.*- 2010.-Vol.46.- P.275–299.
4. Lee, S., & Seo, S.Y. Optimization of yttrium aluminum garnet: Ce<sup>3+</sup> phosphors for white light-emitting diodes by combinatorial chemistry method. *J. Electrochem. Soc.*-2002. – Vol.149.- P. 85–88.
5. Jacobs, R.R., Krupke, W.F., & Weber, M.J. Measurement of excited-state-absorption loss for Ce<sup>3+</sup> in Y<sub>3</sub>Al<sub>5</sub>O<sub>12</sub> and implications for tunable 5d→4f rare-earth lasers. *Applied Physics Letters*. 1978. – Vol.33. –P. 410–415.
6. Ming, L., Ding, Z., Cui P, & Li, Zhe Z. Low temperature molten salt synthesis of YAG:Ce spherical powder and its thermally stable luminescent properties after post-annealing treatment. *Materials Science in Semiconductor Processing*. – 2016. –Vol. – P.101–107.

UDC:371:15

## THE USE OF POSITRON EMISSION TOMOGRAPHY IN MEDICAL PRACTICE

**Tukhtakhodjaeva Feruza Shomansurovna, Abdujabbarova Umida Mashrukovna**

*tuxtaxodjaeva@mail.ru, silver133@gmail.com*

Department of Informatics, biophysics. Tashkent Medical Academy, Tashkent, Uzbekistan  
Research supervisor - I.M.Mullajonov

The imaging method has found application in the study of many biochemical processes. Since in most cases the localization and extent of the pathological process is unknown, the use of an effective diagnostic method throughout the body is a paramount task. Visualization is an extremely effective method for solving this problem, since data is presented in the form of images, namely vision is the most effective system of human perception for search, definition and description. Recognition depends on the type of information presented in the image; both in terms of determining what it means, and in terms of its sensitivity to identify the presence of a pathological process.

In the medical diagnosis of diseases, it often takes a long time before a new imaging technology becomes applicable in clinical practice. For the correct interpretation of the image, many additional studies are necessary. At this stage, positron emission tomography (PET) is now located. In clinical practice, PET has been used since the early nineties and, unlike classical methods (such as computed tomography and magnetic resonance imaging), which allow only images of anatomical structures and changes in them to be obtained, PET allows quantitative analysis of physiological or biochemical functions.

The information obtained from this often reveals many functional changes caused by the disease, long before any morphological changes appear. PET differs from other nuclear medicine research in that PET detects a metabolism in the body's tissues, while other types of nuclear medicine research detect the amount of radioactive material collected in the body's tissue at a specific location in order to examine the function of the tissue.

The first prototype PET scanner appeared in 1952 at the Massachusetts Hospital after six months of design development. He had only two detectors based on sodium iodide located opposite each other and allowed to obtain images based on both the detection of coincidence of events and imbalance. The resolution was low, but the device still allowed to detect the tumor and its spatial